Biosensors and Bioelectronics 24 (2009) 2772–2777

Contents lists available at ScienceDirect

Biosensors and Bioelectronics

journal homepage: www.elsevier.com/locate/bios

Electrochemical biosensor for pesticides based on acetylcholinesterase immobilized on polyaniline deposited on vertically assembled carbon nanotubes wrapped with ssDNA

Subramanian Viswanathan, Hanna Radecka, Jerzy Radecki*

Institute of Animal Reproduction and Food Research, Polish Academy of Sciences, Tuwima 10, 10-747 Olsztyn, Poland

ARTICLE INFO

Article history:
Received 30 October 2008
Received in revised form 26 January 2009
Accepted 30 January 2009
Available online 10 February 2009

Keywords:
Biosensor
Voltammetry
Acetylcholinesterase
Carbon nanotubes
ssDNA
Methyl parathion
Chlorpyrifos

ABSTRACT

An electrochemical biosensor for the determination of pesticides: methyl parathion and chlorpyrifos, two of the most commonly used organophosphorous insecticides in vegetable crops, is described. The self-assembled monolayers (SAMs) of single walled carbon nanotubes (SWCNT) wrapped by thiol terminated single strand oligonucleotide (ssDNA) on gold was utilized to prepare nano size polyaniline matrix for acetylcholinesterase (AChE) enzyme immobilization. The key step of this biosensor was AChE-acetylcholine enzymatic reaction which causes the small changes of local pH in the vicinity of an electrode surface. The pesticides were determined through inhibition of enzyme reaction. The dynamic range for the determination of methyl parathion and chlorpyrifos was found to be in between 1.0×10^{-11} and 1.0×10^{-6} M ($0.6 < SD < 3.5$) with good reproducibility and stability. The detection limit of the biosensor for both pesticides was found to be 1×10^{-12} M. The biosensor has been applied for the determination of methyl parathion and chlorpyrifos in spiked river water samples.

1. Introduction

Organophosphorous pesticides are used widely for agriculture, vector control and domestic purposes as insecticides. The European Union has strictly limited the emissions, discharges and losses of pesticides and has adopted under Decision No. 2451/2001/EC, a list of 33 priority hazardous substances wherein methyl parathion and chlorpyrifos are included (Decision, 2001). Thus, there is a need for fast and inexpensive testing devices for pesticide detection. The integration of biological molecules and nanomaterial transducers has emerged as an effective way of developing nanoscale biosensor devices. The high specificity of biomolecules such as enzymes, receptors and antibodies allows for the assembly of the biosensors which can be used for a wide range of applications. Recently, acetylcholinesterase (AChE) enzyme based biosensors have attracted much attention due to their applications for the detection of anticholinesterase compounds or inhibitors including organophosphate and carbamate pesticides (Istamboulie et al., 2007; Castro et al., 2005; Lin et al., 2005; Schulze et al., 2005; Somerset et al., 2006). AChE belongs to the family of hydrolase characterized by a catalytic triad that is a coordinated structure consisting of three essential amino acids: histidine, serine and aspartic acid (Krasinski et al., 2005; Manetsch et al., 2004). The enzyme catalysis occurs when the triad's anionic binding site attracts the positively charged quaternary ammonium group of acetylcholine. The serine hydroxyl group attacks and cleaves the ester after its deprotonation by a neighboring histidine group in the triad (Woster, 2001). However, in the presence of an inhibitor such as an organophosphate, the nucleophilic serine hydroxyl group located at the active site covalently bound to the phosphorus atom of the organophosphate. Similar reaction occurs with the carbonyl carbon of carbamates and this blocking of the triad serine inactivates the enzyme (Lin et al., 2005; Schulze et al., 2005). Among the biosensing options reported (Singh et al., 1999; Vakurov et al., 2004) for the detection of organophosphate and carbamate pesticides, some of them are based on the principle of inhibition by cholinesterases enzymes (Andreescu et al., 2002; Montesinos et al., 2001; Pogacnik and Franko, 2003). In the presence of an organophosphate or carbamate pesticide, the normal AChE activity is altered resulting in a decrease the response signal of biosensors. This decrease in the sensor response can be related to the pesticide concentration. Various methods employing different enzyme immobilization techniques lead to the attainment of different detection limits in the range from 1 to 400 ng/mL (Kok and Hasirci, 2004; Schulze et al., 2005; Singh et al., 1999).

Carbon nanotubes (CNT) are hollow graphitic cylinders that have recently been explored as a promising material for chemical and biological sensing applications (Zheng et al., 2003; Viswanathan

* Corresponding author. Tel.: +48 89 523 4612; fax: +48 89 524 0124.
E-mail address: radecki@pan.olsztyn.pl (J. Radecki).

0956-5663/$ – see front matter © 2009 Elsevier B.V. All rights reserved.
doi:10.1016/j.bios.2009.01.044

et al., 2006, 2008). Some researchers have reported near single-molecule detection capabilities with CNT-derived conductivity sensors (Roman et al., 2004). One of the challenges is to individually disperse the CNTs, which simplifies their use in sensor fabrications (Pomales and Cabrera, 2007). Functionalization of CNTs by DNA can be achieved with either covalent or non-covalent approaches. Covalent functionalization of the CNTs is usually performed by reacting amino terminated-DNA with the carboxylic acid groups in oxidized CNTs (Liu et al., 2000; Viswanathan et al., 2008). In contrast to the traditional approach of covalently attaching DNA molecules to CNTs, several groups reported the non-covalent functionalization (by means of wrapping) of CNTs by ssDNA in aqueous solutions (Dovbeshko et al., 2003; Dwyer et al., 2002; Zheng et al., 2003). The wrapping of single walled carbon nanotubes (SWCNTs) by ssDNA occurs when the aromatic nucleotide bases in ssDNA may be exposed to form pi-stacking interactions with the hydrophobic side-wall of carbon nanotubes, whereas the hydrophilic part of the ssDNA strand (i.e. the sugar–phosphate backbone) is left exposed to interact with the solvent (Zheng et al., 2003). They also reported that ssDNA binding to CNT converts bund CNT into individual tubes. Another important challenge is the integration of CNTs with solid substrates. Recent reports stated that the formation of a film of ssDNA wrapped CNTs on solid supports for electrochemical application (Hu et al., 2005; Mclean et al., 2006). Reported methods for the vertical attachment of CNTs on solid supports consist of either synthesis-induced alignment (e.g. chemical vapor deposition) (Li et al., 2003; Nguyen et al., 2002) or post-synthesis manipulation (Dai et al., 2003). One of the most interesting approaches for the post-synthesis alignment of CNTs is the self-assembly technique (Gooding et al., 2003; Plank et al., 2004; Rodriguez et al., 2007). Pomales and Cabrera (2007), Pomales et al. (2006) reported the vertical attachment of disulfide modified ssDNA wrapped CNTs on a gold substrate by the self-assembly technique. Nanostructures formed by conducting polymers combined with CNT received great deal of attention due to their properties differ from their bulk structures. CNT-conducting polymer materials offer control properties such as polymer layer thickness, electrical properties and bio-reagent loading, etc. (Manisankar et al., 2005; Viswanathan et al., 2006; Wei and Ivaska, 2006). Polyaniline (PANI) an important conducting polymer is characterized by ease way of preparation, well-behaved electrochemistry, impressive signal amplification, and elimination of electrode fouling when used in biosensor applications (Somerset et al., 2006).

The present work describes the fabrication of a novel electrochemical biosensor by integrating the special features of ssDNA–SWCNT, PANI and AChE for pesticides determination. AChE immobilized on the pH sensitive redox polymer, PANI coated on vertically aliened thiol terminated ssDNA–SWCNTs was used as transducer layer to reach the high sensitivity of this biosensor. Typical pesticides methyl parathion and chlorpyrifos were selected to evaluate the proposed biosensor.

2. Experimental

2.1. Reagents

Acetylcholine chloride (AChCl), acetylcholinesterase (EC 3.1.1.7) from *Electrophorus electricus* (electric eel), bovine serum albumin (BSA), glutaraldehyde, methyl parathion, chlorpyrifos, aniline, single walled carbon nanotubes were purchased from Sigma–Aldrich (St. Louis, USA) and used as received. Pralidoxime chloride (intravenous injection, Ranbaxy, India) was used as received. Thiol terminated single strand DNA with following sequences 5′-HS-TGG GGT TTA-TGG AAA TTG GAA-3′ (ssDNA) was purchased from Institute of Biochemistry and Biophysics (Polish Academy of Sciences, Warsaw, Poland). All other reagents used in this study were of analytical reagent grade. All aqueous solutions were prepared using freshly deionized water (18.2 MΩ cm^{-1} specific resistivity) obtained from Simplicity 185 Water System (Millipore, Molsheim, France).

2.2. Instruments

2.2.1. Electrochemical studies

Electrochemical impedance spectroscopy (EIS), cyclic voltammetry (CV) and square wave voltammetry (SWV) measurements were performed using potentiostat/galvanostat PGSTAT30 (Autolab, Eco Chemie, Utrecht, Netherlands) with a conventional three electrode system comprising platinum wire as auxiliary electrode, Ag/AgCl (3 M NaCl saturated with AgCl) as reference electrode and gold disk electrodes 1.6 mm diameter (Bioanalytical system (BAS), USA) as working electrode. EIS measurements were performed in 0.1 M Na_2SO_4 solution containing $K_3[Fe(CN)_6]/K_4[Fe(CN)_6]$ (0.5 mM each) by applying AC impedance in the frequency range between 0.1 Hz and 100 kHz with a perturbation signal of 5 mV at the formal potential of the redox couple (0.18 V).

2.2.2. Atomic force microscopy

Q-Scope Universal Scanning probe microscope (Ambios Technology, USA) was used to explore the SAMs on gold electrodes at room temperature. Tapping mode was used to acquire the images under ambient conditions.

2.3. Methods

2.3.1. Chemical shortening of CNTs (please refer supplemental information)

2.3.1.1. ssDNA–CNT hybrids preparation. ssDNA wrapped SWCNTs were prepared according to the previously reported procedure (Zheng et al., 2003). In this method, 1 mg of shortened SWCNTs were mixed with 500 μL of 1 μM ssDNA in 0.05 M PBS containing 0.1 M NaCl and sonicated for 1 h in an ice bath. Subsequent centrifugation for 30 min at 5000 rpm was used to remove insoluble materials from the dispersion. Finally, the dispersion was stored at 4 °C. The precipitation was not occurred even after storing for one month.

2.3.2. Electrode cleaning (please refer supplemental information)

2.3.2.1. Self-assembled monolayers. Self-assembled monolayers were formed by immersing clean gold electrodes in 200 μL of ssDNA (0.1 μM/mL) or ssDNA–SWCNT (∼0.2 mg/mL) in 0.05 M PBS containing 0.1 M NaCl (pH 7.0) for the period of 24 h at 4 °C. After the immobilization period, the electrodes were removed from the solution, rinsed with milliQ water, and dried with argon stream.

2.3.3. Preparation of samples for AFM studies (please refer supplemental information)

2.3.3.1. Electrochemical polymerization of aniline. Electrochemical polymerization of aniline on the electrode surface was achieved by applying potential cycling between 0.0 and 0.95 V at a scan rate of 100 mV/s to 0.05 M aniline solution in 0.1 M PBS, pH 3.5. Approximately 10 cycles were sufficient to deposit PANI on the electrode surface.

2.3.4. AChE enzyme immobilization

According to Sigma–Aldrich product information 0.02 M PBS pH 7.0 was used for 0.01 mg/mL AChE enzyme solution as optimum. First, the electrodes were immersed in glutaraldehyde aqueous solution for 30 min, then, 10 μL of 0.01 mg/mL AChE in 0.02 M (pH 7.0) PBS were dropped on the electrode surfaces and allowed to incubate for 30 min at 4 °C. To block the nonspecific binding

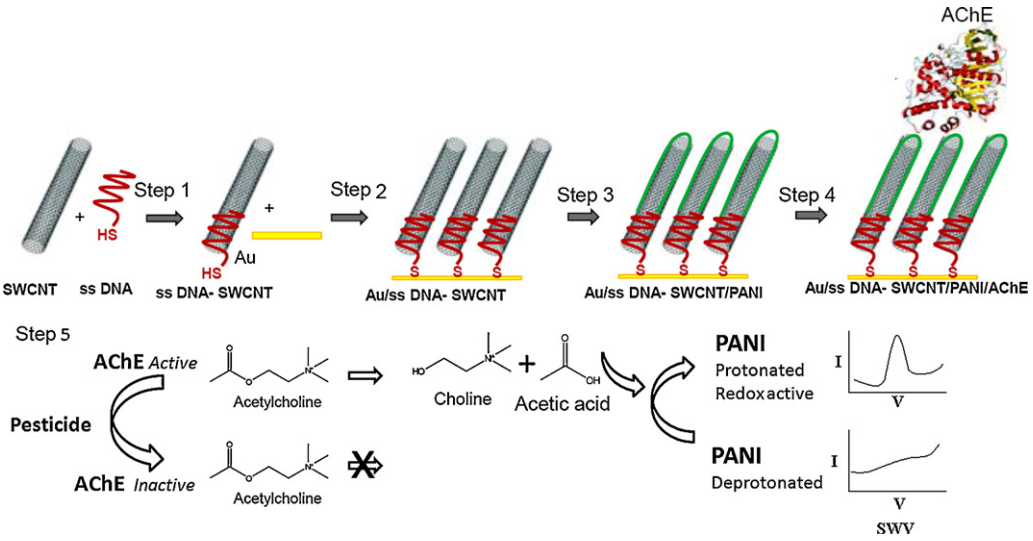

Fig. 1. Schematic representation of biosensor fabrication and its functions. Step 1 – SWCNT wrapping with thiol terminated ssDNA; Step 2 – ssDNA wrapped SWCNT self-assembled on gold electrode; Step 3 – controlled electrochemical polymerization of aniline on the Au/ssDNA–SWCNT layers; Step 4 – immobilization of AChE enzyme by glutaraldehyde; Step 5 – pesticide sensing mechanism of Au/ssDNA–SWCNT/PANI/AChE.

sites, the electrodes were incubated with 100 μL of 0.01 mg/mL BSA in 0.1 M PBS (pH 7.0), for 30 min at 4 °C. Finally, the electrode was washed with 0.1 M PBS buffer pH 7.0 and stored at 4 °C.

2.3.5. Enzyme assay procedure

Polypropylene hollow cylinder tightly fitted on the top of BAS Au electrode was used as the electrochemical cell. Two hundred microlitres of the electrolyte was required for each experiment. Voltammetric measurements were made after optimum period of incubation (15 min) with electrolyte. PBS (0.002 M, 0.1 M NaCl, pH 7.0) solution containing optimum amount of AChCl (1 mM) was added into the cell for control experiment. To measure the inhibition, the pesticide solution (methyl parathion or chlorpyrifos) was mixed and added to the cell. The decrease in current due to the addition of pesticide solution was recorded. Deactivated AChE enzyme on the electrode was reactivated with 1 mg/mL pralidoxime chloride for 15 min. Then the electrode was tested in electrochemical cell of 200 μL with 0.002 M PBS (pH 7.0) containing 1 mM AChCl to measure the electrochemical responses. River water samples were collected from middle stream of local river at Olsztyn, Poland. All samples were filtered, centrifuged 13,000 rpm for 30 min and used for recovery studies.

3. Results and discussions

A schematic representation of the biosensor obtained in our experiments and the procedures used for its preparation is shown in Fig. 1. At each step of modification, the electrode surfaces were characterized by either AFM or electrochemical methods.

3.1. AFM studies

Atomic force microscopy in tapping mode was used to characterize the ssDNA–SWCNT SAMs. AFM image of Au/ssDNA SAM and Au/ssDNA–SWCNT SAMs is depicted in Fig. 2. Au/ssDNA SAM surface image (supplemental Fig. S1) has been shown with a average height of 6–8 nm, which can be assigned to ssDNA which is in good agreement with the 7.14 nm value predicted for ssDNA sequence used (21-mer). After ssDNA–SWCNT SAM formation, needlelike protrusions are clearly seen on the gold surface (Fig. 2). The image shows aggregates, with an average height of 500 nm. The average height of protrusions is much higher than the value for ssDNA strands. From these observations, we can conclude that the thiol terminated ssDNA–SWCNT have been successfully immobilized on gold via Au–S chemical bonding, with the nanotubes vertically aligned on the gold surface.

3.2. EIS analysis

Electrochemical impedance spectroscopy measurements were carried out to compare the characteristics of ssDNA and ssDNA–SWCNT SAMs on gold. Fig. 3 shows Nyquist plots and equivalent circuits. The equivalent circuits, $R_1(Q_1[R_2(R_3Q_2)])$, for Au/ssDNA–SWCNT and $R_1(Q_1[R_2W])$, for Au/ssDNA were applied for fitting analysis. Au/ssDNA–SWCNT behaved like porous electrode. The angle of the line in semi-infinite region was observed less than 45°. This is typical for porous electrodes. The diameter of the semicircle corresponds to the interfacial charge transfer resistance (R_{ct}), which usually represents the resistance of faradaic reactions on the electrode (Bard and Faulkner, 2001). Obviously, the R_{ct} of ssDNA–SWCNT SAM is much lower than that of ssDNA SAM. The above EIS results revealed that ssDNA–SWCNT SAM has an obvious improvement effect for a faster charge transfer rate than with plain ssDNA SAMs.

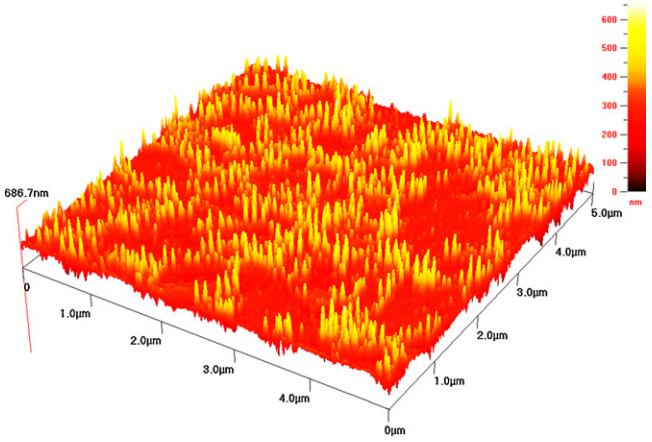

Fig. 2. Typical AFM images of ssDNA wrapped SWCNT SAMs on Au(1 1 1) surface.

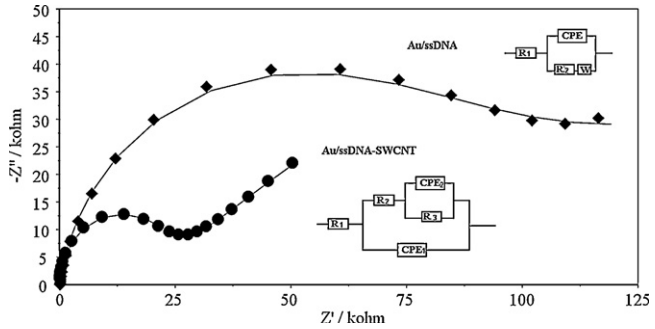

Fig. 3. Electrochemical impedance Nyquist plot of Au/ssDNA SAM and Au/ssDNA–SWCNT SAM at 0.1 M Na_2SO_4 containing 0.5 mM $K_3[Fe(CN)_6]$ and 0.5 mM $K_4[Fe(CN)_6]$. Inset: circuit model, R_1, R_2 and R_3 – resistance, CPE, CPE_1 and CPE_2 – constant phase element.

3.3. Electrochemical polymerization

Electrochemical polymerization was used for the preparation of PANI nanostructures on Au/ssDNA–SWCNT SAMs. Both the polymer deposition and electrode surface morphology were determined by ssDNA–SWCNT SAMs. Electrochemical polymerization of aniline on Au/ssDNA–SWCNT SAMs were achieved in aqueous 0.1 M PBS at pH 3.5 in the potential range described in experimental section. As reported previously, the redox process corresponds to electron transfer of the electrodeposited PANI film (Somerset et al., 2006; Wei and Ivaska, 2006).

Multi-cycle CV results showed an increase in the redox peak currents indicating the growth of conducting polymer film with every cycle completed. The large currents observed at the positive end of the CV are due to the oxidation of aniline monomer and oxidation of the PANI film (Fig. S2). Ten scan cycles was optimum to make thin PANI deposition on Au/ssDNA–SWCNT but higher numbers of scan cycles yielded rapid growth of PANI film and nanostructures were completely buried in PANI films. PANI redox peaks can be attributed to the electron transitions between the redox states of leucoemeraldine and pernigraniline (Prakash, 2002). The formal potential for the redox couple was calculated to be 300 ± 30 mV (Fig. S3). It is well documented that PANI redox behavior depends on pH (Malhotra et al., 2006). The enzyme based reactions generate pH changes in their local environments through their byproducts (Skotheim and Reynolds, 2007). The pH-dependence of PANI appears to be of crucial importance due to the potential use of this polymer for amperometric biosensors. Fig. 1 shows the schematic representation of the enzyme reactions of the biosensor system. Acetylcholine hydroxylation produced the byproducts acetic acid and choline. The acetic acid molecules diffused into the electrode surface. The self-assembled ssDNA–SWCNT supported PANI nanostructures acted as proton collecting antennas on the electrode surface and resulting in protonation of PANI films. The changes in the redox activity of the PANI directly related to the pH. High surface area of self-assembled ssDNA–SWCNT supported polyaniline nanostructures served dual role as pH sensitive layer and support for AChE immobilization.

3.4. Optimization of biosensor for pesticides determination

Cross-linking with glutaraldehyde is the most widely used method for AChE immobilization on electrochemical sensors (Gallego et al., 2005; Arora et al., 2007). However, poor reproducibility and significant loss of enzyme activity were observed when glutaraldehyde was used in excess. To study the effect of glutaraldehyde concentration on AChE immobilization, electrodes were fabricated using different concentrations of glutaraldehyde and corresponding SWV net currents (difference between forward and reverse waves) responses were measured at PBS (0.002 M, 0.1 M NaCl, pH 7.0) containing 2.0 mM AChCl (Fig. S4). The biosensor responses depended on the buffer capacity of the working solution. Strong buffer concentration neutralizes the acetic acid molecule. Therefore 0.002 M PBS containing 0.1 M NaCl was selected to observe biosensor responses. An amount of less than 2% (w/w) glutaraldehyde was found to be insufficient to bind all enzyme molecules on the transducer surface. On the other hand, a decrease in the enzyme activity was observed for solutions containing glutaraldehyde concentration higher than 2% (w/w). A possible explanation could be a high degree of enzyme reticulation and consequent restrained access of substrate to enzyme active center. From the above results 2% (w/w) glutaraldehyde concentration was selected as optimum for further experiments.

Next the concentration of AChCl was optimized. The SWVs of Au/ssDNA–SWCNT/PANI/AChE in the cell solution containing AChCl substrate was performed under anaerobic conditions. Fig. 4 shows well defined current response of the biosensor at 1.0 mM AChCl concentration. In the absence of AChCl, the peak responses were negligible. The SWV net current responses were plotted against concentrations of AChCl (Fig. S5). Voltammetric measurements were performed after each addition of the AChCl up to a maximum concentration of 1.6 mM. The SWV peak currents were found to increase with the concentration of AChCl up to 1.0 mM. There was no significant SWV current improvement for 1.0–1.6 mM of AChCl concentration and this revealed that the electrode had reached its saturation level. From the above results, 1.0 mM of AChCl was selected as optimum concentration for further experiments. The interactions of AChCl on enzyme free electrode were also studied. In this case, SWV responses of Au/ssDNA–SWCNT/PANI were measured with increasing the concentration of AChCl up to 1.6 mM. There were no noticeable changes on enzyme-free Au/ssDNA–SWCNT/PANI electrode. It indicated the biosensor responses only related with the enzyme reactions. Optimization of incubation period for biosensor with substrate was studied between 0 to 30 min and 15 min was found as optimum value.

The biosensor prepared under optimum working conditions was tested with respect to its stability in 1.0 mM of AChCl in 0.002 M PBS (pH 7.0). A total of 10 measurements were taken during 5-day period of time. The electrodes were kept in 0.002 M PBS (pH 7.0) and stored at 4 °C in the refrigerator. The responses of the electrodes showed a maximum value within the first few days and then began to decrease. After 5 days, they reached a constant value of about ~86% of their initial response (Fig. S6).

The performance of ssDNA–SWCNT SAM in the proposed biosensor was compared with AChE immobilized on PANI electropolymerized on bare Au (Au/PANI/AChE) and AChE immobilized on PANI electropolymerized on dip coated SWCNT/Au (please refer

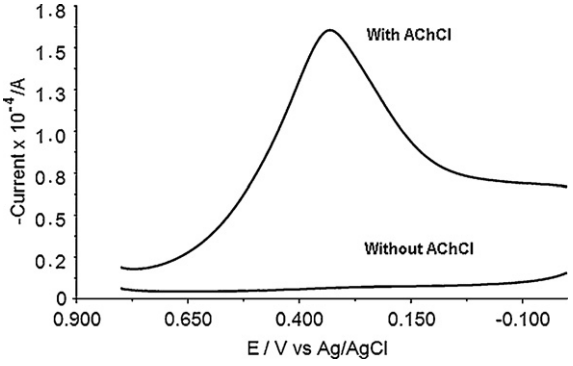

Fig. 4. SWV net current responses of biosensor with and without AChCl; SWV measuring conditions: SWV frequency 25 Hz, amplitude 100 mV and step potential 1 mV.

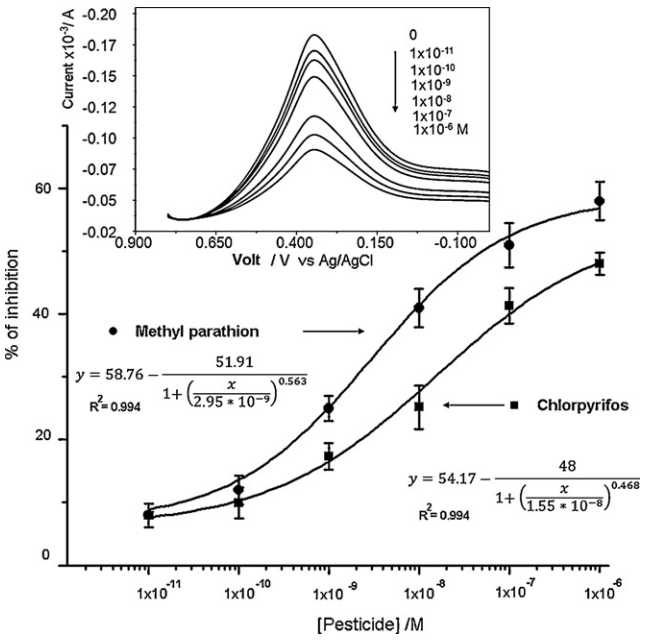

Fig. 5. Calibration curve for methyl parathion and chlorpyrifos (0.6<SD < 3.5); inset figure: SWV net current responses of biosensor after 15 min incubation with different concentrations of methyl parathion in 0.002 M PBS (pH 7.0) containing 1 mM AChCl and 0.1 M NaCl; SWV measuring conditions. Refer Fig. 4.

supplemental information for electrode modification procedure) (Au/SWCNT/PANI/AChE) under identical experimental conditions. Supplemental Fig. S7 compares the SWV response of Au/PANI/AChE, Au/SWCNT/PANI/AChE and Au/ssDNA–SWCNT/PANI/AChE at 1 mM AChCl at optimized conditions. The current response for Au/ssDNA–SWCNT/PANI/AChE was highest among the three electrodes. The above results indicated that the ssDNA–SWCNT SAM improved the electrode surface quality for biosensor fabrication and function.

3.5. Pesticides determination

Methyl parathion and chlorpyrifos pesticides are known to inhibit the reaction between AChE and acetylcholine. Inhibition measurements were performed in conditions corresponding to saturation of the enzymatic layer with the substrate 1.0 mM of AChCl concentration. In saturated conditions, the decreases in biosensor SWV responses after contact with pesticide solution is related only to the enzyme–inhibitor interaction and does not depend on the mass transfer of both the substrate and the inhibitor from the bulk solution to the enzymatic layer. The SWV responses were associated with inhibition of the enzyme activity by amount pesticide added (inset Fig. 5). The decreasing of redox peak current can be explained as the result of the blocking of serine hydroxyl group by covalently bound phosphate group, which invariably reduces the overall charge of the catalytic active site (Krasinski et al., 2005). The percentage inhibition of the biosensor can be calculated with Eq. (1):

$$\text{Inhibition}\,(\%) = [(I_0 - I_s)/I_0] \times 100 \quad (1)$$

Where I_0, I_s were the peak currents of 1.0 mM of acetylcholine in 0.002 M PBS buffer with 0.1 M NaCl without and with pesticides inhibition respectively. Plots of the percentage inhibition of the biosensor as a function of pesticide concentration are shown in Fig. 5. SWV peak currents were found to decrease with increase of parathion concentration from 1.0×10^{-11} up to 1.0×10^{-6} M with correlation coefficient r^2 0.994. Bioassays with a quantitative response showing a sigmoid log–dose relationship can be analyzed by fitting a non-linear dose–response model directly to the data. Logistic regression yields accurate quantization across a wider range of concentrations compared to linear regression. It is demonstrated that the four-parameter logistic (4PL) model, previously reported (Baud, 1993; Healy, 1972; O'Connell et al., 1993) could be applied to this bioassay. The 4PL regression of a standard curve for pesticides determination, with the log of the concentration of pesticide plotted on the *x*-axis and the response (percentage of inhibition) plotted on the *y*-axis, is presented in Fig. 5. Once a 4PL equation is created from a set of data, values for all four of the parameters will be determined.

$$y = b + \frac{a - b}{1 + \left(\frac{x}{c}\right)^d} \quad (2)$$

where a is the response at zero concentration, b is the response at maximum concentration, x is pesticide concentration in M, c is the concentration yielding 50% response, d is a slope factor (Viswanathan et al., 2008). Similar results were obtained for the chlorpyrifos pesticide. The detection limits were determined by lowest analytical response which was three times higher than the standard deviation of 10 measurements done in the absence of pesticide. The detection limit was found to be 1×10^{-12} M for methyl parathion and chlorpyrifos.

3.6. Reactivation of the biosensor

Phosphorylated AChE, when bound to organophosphorous pesticides, undergoes hydrolytic regeneration at a slow or negligible rate. Oximes, which are nucleophilic agents, act as chemical 'reactivators' of AChE via a nucleophilic attack at the phosphorylated enzyme, enabling the release of pesticides from AChE. Pralidoxime chloride reactivates AChE a million times more rapidly than the spontaneous release of the bound organophosphate compound. AChE inhibited by organophosphorous pesticides can be completely reactivated by use of nucleophilic compounds such as pralidoxime chloride (Weinbroum, 2005; Du et al., 2007). The reactivation efficiency was estimated as follows:

$$\text{Reactivation}\,(\%) = (I_a - I_s/I_0 - I_s) \times 100 \quad (3)$$

where I_a was the peak current of AChCl on Au/ssDNA–SWCNT/PANI/AChE after pralidoxime chloride reactivation and I_0, I_s were the peak currents of 1.0 mM of acetylcholine in 0.002 M PBS (pH 7.0) with 0.1 M NaCl without and with pesticides inhibition respectively. It was observed that AChE biosensor inhibited by pesticides could resume 90% original activity after incubation with 1 mg/mL pralidoxime chloride. With increasing incubation time, the reactivation efficiency increased and reached a constant value after 15 min (Fig. S8). The proposed reactivation procedure for this biosensor could be used repeatedly with an acceptable reproducibility.

Table 1
Recovery studies of methyl parathion and chlorpyrifos in river water samples under optimum conditions.

Pesticides	Added (M)	Found (M)	% of recovery	SD (n = 5)
Methyl parathion	1.0×10^{-7}	1.07×10^{-7}	107	3.4
	1.0×10^{-8}	9.6×10^{-9}	95	4.5
	1.0×10^{-9}	9.0×10^{-10}	90	4.6
	1.0×10^{-10}	8.9×10^{-11}	89	5.4
Chlorpyrifos	1.0×10^{-7}	9.1×10^{-8}	91	4.1
	1.0×10^{-8}	9.6×10^{-9}	96	4.9
	1.0×10^{-9}	1.1×10^{-9}	110	2.4
	1.0×10^{-10}	8.9×10^{-11}	87	5.7

3.7. Recovery studies

To further demonstrate the applicability of the proposed biosensor, the recovery test was studied by adding pesticides into river water samples. The results are presented in Table 1. The recovery percentages were found to vary from 87% to 110%. This indicated that the proposed biosensor can be used for trace level detection of pesticides present in relevant samples.

4. Conclusions

The proposed vertically aliened ssDNA–SWCNT SAMs coated with thin PANI film on gold electrodes demonstrated superior charge transport properties than the ssDNA SAMs. The incorporation of SWCNTs not only provided the conductive pathways to promote the electron transfer, but also increased the surface area of flexible three-dimensional conductive supports for acetylcholinesterase enzyme. Thin PANI film on SWCNT acted as good sensor for enzyme byproduct acetic acid. The changes of local pH in the vicinity of an electrode surface by enzymatic reaction increases the redox activity of PANI thin film on SWCNTs. The pesticides were determined with the proposed biosensor through the enzyme inhibition mechanism. The biosensor was successfully tested in the determination of two common pesticides such as methyl parathion and chlorpyrifos, which belongs to the organophosphorous family. The detection limit was found to be 1×10^{-12} M for methyl parathion and chlorpyrifos which is lower than the maximum contaminant level recommended by the European Environmental Bureau and other environmental protection agencies. The proposed transducer layer can be used as a suitable base for biosensors based on enzymes which can release acidic or basic byproducts.

Acknowledgements

The authors gratefully acknowledge European Union Marie Curie Transfer of Knowledge Research Grant MTKD–CT-2006-042708, Polish Ministry of Sciences and Higher Education No. 105/6.PR UE/2007/7 and statutory funds of Institute of Animal Reproduction and Food Research of Polish Academy of Science, Olsztyn, Poland.

Appendix A. Supplementary data

Supplementary data associated with this article can be found, in the online version, at doi:10.1016/j.bios.2009.01.044.

References

Andreescu, S., Noguer, T., Magearu, V., Marty, J.L., 2002. Talanta 57, 169–176.
Arora, K., Sumana, G., Saxena, V., Gupta, R.K., Gupta, S.K., Yakhmi, J.V., Pandey, M.K., Chand, S., Malhotra, B.D., 2007. Anal. Chim. Acta 594, 17–23.
Bard, A.J., Faulkner, L.R., 2001. Electrochemical Methods: Fundamentals and Applications, second ed. Wiley, New York.
Baud, M., 1993. In: Masseyeff, R.F., Albert, W.H., Staines, N.A. (Eds.), Methods of Immunological Analysis, vol. 1. VCH Weinheim.
Castro, B.I.R., Contes, E.J., Davis, M.E.P., Cabrera, C.R., 2005. Rev. Adv. Mat. Sci. 10, 381–386.
Dai, L., Patil, A., Gong, X., Guo, Z., Liu, L., Liu, Y., Daoben, Z., 2003. Chem. Phys. Chem. 4, 1150–1169.
Decision No. 2455/2001/EC of the European Parliament and of the Council of 20 November 2001. Establishing the list of priority substances in the field of water policy and amending Directive 2000/60/EC. Off. J. Eur. Commun. L331, 15/12/2001, 1–5.
Dovbeshko, G.I., Repnytska, O.P., Obraztsova, E.D., Shtogun, Y.V., 2003. Chem. Phys. Lett. 372, 432–437.
Du, D., Huang, X., Cai, J., Zhang, A., 2007. Biosens. Bioelectron. 23, 285–289.
Dwyer, C., Guthold, M., Falvo, M., Washburn, S., Superfine, R., Erie, D., 2002. Nanotechnology 13, 601–604.
Gallego, F.L., Betancor, L., Mateo, L., Hidalgo, A., Morales, N.A., Ortiz, G.D., Guisan, J.M., Lafuente, R.F., 2005. J. Biotechnol. 119, 70–75.
Gooding, J.J., Wibowo, R., Liu, J.Q., Yang, W., Losic, D., Orbons, S., Mearns, F.J., Shapter, J.G., Hibbert, D.B., 2003. J. Am. Chem. Soc. 125, 9006–9007.
Healy, M.J.R., 1972. Biochem. J. 130, 207–210.
Hu, C., Zhang, Y., Bao, G., Zhang, Y., Liu, M., Wang, Z.L., 2005. J. Phys. Chem. B 109, 20072–20076.
Istamboulie, G., Andreescu, S., Marty, J.-L., Noguer, T., 2007. Biosens. Bioelectron. 23, 506–512.
Kok, F.N., Hasirci, V., 2004. Biosens. Bioelectron. 19, 661–665.
Krasinski, A., Radic, Z., Manetsch, R., Raushel, J., Taylor, P., Sharpless, K.B., Kolb, H.C., 2005. J. Am. Chem. Soc. 127, 6686–6692.
Li, J., Ng, H.T., Cassell, A., Fan, W., Chen, H., Ye, Q., Koehne, J., Han, J., Meyyappan, M., 2003. Nano Lett. 3, 597–602.
Lin, G., Lee, Y.R., Liu, Y.C., Wu, Y.G., 2005. Chem. Res. Toxicol. 18, 1124–1131.
Liu, Z., Shen, Z., Zhu, T., Hou, S., Ying, L., Shi, Z., Gu, Z., 2000. Langmuir 16, 3569–3573.
Malhotra, B.D., Chaubey, A., Singh, S.P., 2006. Anal. Chim. Acta 578, 59–74.
Manetsch, R., Krasinski, A., Radic, Z., Raushel, J., Taylor, P., Sharpless, K.B., Kolb, H.C., 2004. J. Am. Chem. Soc. 126, 12809–12818.
Manisankar, P., Viswanathan, S., Pusphalatha, A.M., Rani, C., 2005. Anal. Chim. Acta 528, 157–163.
Mclean, R.S., Huang, X., Khripin, C., Jagota, A., Zheng, M., 2006. Nano Lett. 6, 55–60.
Montesinos, T., Peřrez-Munguia, S., Valdez, F., Marty, J.L., 2001. Anal. Chim. Acta 431, 231–237.
Nguyen, C.V., Delzeit, L., Cassell, A.M., Li, J., Han, J., Meyyappan, M., 2002. Nano Lett. 2, 1079–1081.
O'Connell, M.A., Belanger, B.A., Haaland, P.D., 1993. Chemom. Intell. Lab. Syst. 20, 97–114.
Plank, N.O.V., Cheung, R., Andrews, R.J., 2004. Appl. Phys. Lett. 85, 3229–3231.
Pogacnik, L., Franko, M., 2003. Biosens. Bioelectron. 18, 1–9.
Pomales, G.S., Cabrera, C.R., 2007. J. Electroanal. Chem. 606, 47–54.
Pomales, G.S., Rivera-Vélez, N.E., Cabrera, C.R., 2006. ECS Trans. 3, 21–29.
Prakash, R., 2002. J. Appl. Polym. Sci. 83, 378–385.
Rodriguez, L.S., Pomales, G.S., Pagan, A.R., Cabrera, C.R., 2007. ECS Trans. 3, 15–26.
Roman, C., Ciontu, F., Courtois, B., 2004. Nanotechnology 16, 263–266.
Schulze, H., Muench, S.B., Villatte, F., Schmid, R.D., Bachmann, T.T., 2005. Anal. Chem. 77, 5823–5830.
Singh, A.K., Flounders, A.W., Volponi, J.V., Ashley, C.S., Wally, K., Schoeniger, J.S., 1999. Biosens. Bioelectron. 14, 703–713.
Skotheim, T.A., Reynolds, J.R. (Eds.), 2007. Handbook of Conducting Polymers, third ed. Taylor & Francis Group, LLC, FL, USA.
Somerset, V.S., Klink, M.J., Sekota, M.M.C., Baker, P.G.L., Iwuoha, E.I., 2006. Anal. Lett. 39, 1683–1698.
Vakurov, A., Simpson, C.E., Daly, C.L., Gibson, T.D., Millner, P.A., 2004. Biosens. Bioelectron. 20, 1118–1125.
Viswanathan, S., Wu, L.C., Huang, M.R., Ho, J.A., 2006. Anal. Chem. 78, 1115–1121.
Viswanathan, S., Rani, C., Anand, A.V., Ho, J.A., 2008. Biosens. Bioelectron. 24, 1984–1989.
Wei, D., Ivaska, A., 2006. Chem. Anal. (Warsaw) 51, 839–852.
Weinbroum, A.A., 2005. Brit. Med. Bull. 72, 119–213.
Woster, P.M., 2001. Pharmaceutical Biochemistry. HarperCollins Publishers Inc., New York, USA.
Zheng, M., Jagota, A., Semke, E.D., Diner, B.A., Mclean, R.S., Lustig, S.R., Richardson, R.E., Tassi, N.G., 2003. Nat. Mater. 2, 338–342.